REPORT DOCUMENTATION PAGE

Form Approved
OMB No. 0704-0188

1. REPORT DATE *(DD-MM-YYYY)*	2. REPORT TYPE	3. DATES COVERED *(From - To)*
	Technical Papers	

4. TITLE AND SUBTITLE

Please see attached

5a. CONTRACT NUMBER

5b. GRANT NUMBER

5c. PROGRAM ELEMENT NUMBER

6. AUTHOR(S)

5d. PROJECT NUMBER
1011

5e. TASK NUMBER
CA9F

5f. WORK UNIT NUMBER
34616 1

7. PERFORMING ORGANIZATION NAME(S) AND ADDRESS(ES)

Air Force Research Laboratory (AFMC)
AFRL/PRS
5 Pollux Drive
Edwards AFB CA 93524-7048

8. PERFORMING ORGANIZATION REPORT

9. SPONSORING / MONITORING AGENCY NAME(S) AND ADDRESS(ES)

Air Force Research Laboratory (AFMC)
AFRL/PRS
5 Pollux Drive
Edwards AFB CA 93524-7048

10. SPONSOR/MONITOR'S ACRONYM(S)

11. SPONSOR/MONITOR'S NUMBER(S)
Please see attached

12. DISTRIBUTION / AVAILABILITY STATEMENT

Approved for public release; distribution unlimited.

13. SUPPLEMENTARY NOTES

14. ABSTRACT

15. SUBJECT TERMS

16. SECURITY CLASSIFICATION OF:			17. LIMITATION OF ABSTRACT	18. NUMBER OF PAGES	19a. NAME OF RESPONSIBLE PERSON
a. REPORT	b. ABSTRACT	c. THIS PAGE			Leilani Richardson
Unclassified	Unclassified	Unclassified	A		19b. TELEPHONE NUMBER *(include area code)* (661) 275-5015

10 11 CA 91

MEMORANDUM FOR PRS (In-House Publication)

FROM: PROI (STINFO) 28 February 2002

SUBJECT: Authorization for Release of Technical Information, Control Number: **AFRL-PR-ED-TP-2002-044**
Timothy Miller (PRSM), E. Guan (SUNY Stonybrook), "An Experimental Investigation of Interfacial Fracture Augmented by Modeling and Simulation"

Society for Experimental Mechanics 2002 Ann. Conf. **(Statement A)**
(Milwaukee, WI, 10-12 June 2002) (Deadline: 22 Mar 2002)

1. This request has been reviewed by the Foreign Disclosure Office for: a.) appropriateness of distribution statement, b.) military/national critical technology, c.) export controls or distribution restrictions, d.) appropriateness for release to a foreign nation, and e.) technical sensitivity and/or economic sensitivity.
Comments:_____

Signature _____ Date _____

2. This request has been reviewed by the Public Affairs Office for: a.) appropriateness for public release and/or b) possible higher headquarters review.
Comments: _____

Signature _____ Date _____

3. This request has been reviewed by the STINFO for: a.) changes if approved as amended, b) appropriateness of references, if applicable; and c.) format and completion of meeting clearance form if required
Comments:_____

Signature _____ Date _____

4. This request has been reviewed by PR for: a.) technical accuracy, b.) appropriateness for audience, c.) appropriateness of distribution statement, d.) technical sensitivity and economic sensitivity, e.) military/ national critical technology, and f.) data rights and patentability
Comments:_____

APPROVED/APPROVED AS AMENDED/DISAPPROVED

_____

PHILIP A. KESSEL Date
Technical Advisor
Space and Missile Propulsion Division

AN INVESTIGATION OF INTERFACIAL FRACTURE USING EXPERIMENTS, MODELING, AND SIMULATION

T. C. Miller
Air Force Research Lab
10 E. Saturn Blvd.
Edwards AFB, CA 93524*

E Guan
State University of New York
Dept. of Mechanical Engineering
Stony Brook, NY 11794

Joseph Todaro
State University of New York
Dept. of Mechanical Engineering
Stony Brook, NY 11794

ABSTRACT

The behavior of a bimaterial specimen consisting of a rubbery particulate composite with a thin rubber layer is studied experimentally and computationally. The purpose of the investigation is to study the behavior so fracture in the rubber material can be understood better. The paper uses computer-aided speckle interferometry to interrogate specimens deformed using tensile testing. Computational modeling of the specimens is also addressed. Key findings are different behavior for the two materials, the presence of an intermediate region, and delamination sites that are dependent on specimen geometry.

INTRODUCTION

Modern rocket propulsion had beginnings with pioneer Robert Goddard. Although Goddard had many motor failures, the scale and expense of today's rocket motors is massive by comparison, and the additional complexity of the modern rocket system provides multiple possibilities for failure, any one of which could result in lost lives and large capital losses. One failure mode involves deterioration of the layered materials near the inside of the rocket motor case.

From the outside in, the typical large solid rocket motor has an outer casing, an insulator layer, a rubber liner layer, and an inner core of solid rocket propellant, a composite composed of a high volume fraction of hard particles embedded in a rubber matrix and referred to as a rubbery particulate composite (RPC).[1, 2, 3] Each layer has its own peculiar mechanical characteristics. Although they contribute to the motor performance in some significant way, each material adds complexity and increases the number of potential failure locations. One area that has caused problems is near the liner-propellant interface. The region near this interface can have defects originating and evolving during the manufacturing, storing, handling, or launching of the rocket. Typically, this type of failure is investigated using fracture mechanics, although the effects of the interfaces on these fractures are not well understood.

This work is part of an ongoing effort to understand this phenomenon. We hope a thorough examination of the simplified experiments conducted here will provide useful insights into interfacial mechanics in general, and in particular to the rocket motor problem. These initial experiments use a combination of speckle interferometry and computational modeling to examine a bimaterial specimen without cracks. More detailed future experiments will use these results as a foundation.

EXPERIMENTAL PROCEDURE

We performed the experiments using a tensile testing machine to deform the bimaterial specimens while simultaneously capturing images using a charge-coupled device (CCD) camera. Later, these specimen images were analyzed using the Computer-Aided Speckle Interferometry (CASI) method. Additionally, we used the images to determine the displacement of the specimen edges and the two rubber-RPC interfaces. These displacements were the basis for the average strain measurements and the associated strain rate measurements shown later in the Discussion section.

A typical specimen is shown in Figure 1. The specimen is composed of two materials, with the rubber material sandwiched between the rubbery particulate composite and adhered using a thin layer of urethane adhesive. By using a thin layer of adhesive we hoped to minimize its effects while avoiding another complication: the migration of material constituents across the interface caused by co-curing of the materials. The thin rubber layer is also used in the motor, which has a layer of comparable thickness next to the RPC layer. In the actual application, layers of other materials are present, and instead of adhesive the use of co-curing of the materials is employed. A more comprehensive model that incorporated these features (i.e., co-curing and incorporation of the case and insulator layers) is possible. However, we thought the extra complexities would make the problem intractable.

We glued the specimen into the two aluminum grips and pulled them with a screw driven tensile testing machine. The grips can be considered rigid compared with the specimen materials and are used to apply uniform displacements to the specimen edges. For the specimen shown the dimensions are: Thickness = 5.1 mm, Overall Height = 101.6 mm, and Width = 25.4 mm. The rubber layer has a height of 2.5 mm. Specimen width was varied in the experiments with several trials conducted for each thickness, as shown in Table 1. For the figures shown in the Discussion section, the results are for a specimen with a width of 25.4 mm.

The experimental procedure has been given in general. More specifically, the specimens were deformed using a screw driven tensile testing machine with a crosshead speed of 0.25 mm/min using the aluminum end tabs shown in Figure 1, giving uniform displacements along the top and bottom edges of the bima-

*Approved for public release; distribution unlimited

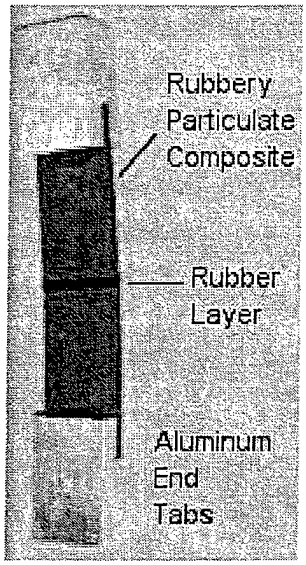

Figure 1: Bimaterial Specimen in End Tabs

Table 1: Specimen Test Matrix

Specimen Width [mm]	Specimens Tested
25.4	2
12.7	9
5.1	2

terial specimens. The images were captured in real time and analyzed later using the CASI method. This is a computational approach of speckle photography that measures two-dimensional displacements well using a CCD camera and Fourier spectrum analysis.[4, 5, 6]

Although two-dimensional contour maps of both in-plane displacement components were obtained, for this initial finding the method was used to find the vertical displacement components as a function of position. The derivative of this displacement component with respect to the vertical coordinate can then be used to determine the normal strain in the vertical direction, ϵ_{yy}. The CCD images were also used to determine the relative displacements of the two interfaces and the specimen top and bottom edges, giving average strain values. These were then used to calculate strain rates as a function of time using a simple finite difference formula (see Equation 5 below). Average strains in both the rubber and RPC layers are given by the equations below using the notation in Figure 2 (superscripts on strain indicate Eulerian or Lagrangian strain). The displacement profile is used with the average strain measures to determine the bimaterial specimen behavior.

$$\epsilon^L_{RPC} = d_1/L \quad (1)$$

$$\epsilon^L_{rubber} = (d_2 - d_1)/l \quad (2)$$

$$\epsilon^E_{RPC} = d_1/(L + d_1) \quad (3)$$

$$\epsilon^E_{rubber} = (d_2 - d_1)/(l + d_2 - d_1) \quad (4)$$

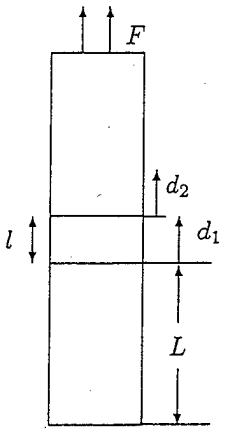

Figure 2: Notation Used for Average Strain Determinations (Not to Scale)

$$\dot{\epsilon}(t = t_i) = \frac{\epsilon_{t_{i+1}} - \epsilon_{t_{i-1}}}{t_{i+1} - t_{i-1}} \quad (5)$$

The data was collected for up to 34 minutes, although delaminations occurred after about 5-6 minutes. Consequently, most of the modeling efforts were focused on the first several minutes of deformation. The experimental method, used in this way, gave us information on the uniformity of strain as well as the average strains and strain rates as a function of time. We used this data for comparison of the computational model with the experiments to assess the success of the modeling effort.

We performed additional experiments on bulk specimens solely to determine the constitutive properties for the computational modeling effort. The specimens were cut either from rubber sheets (for the rubber specimens) or from blocks of RPC material. The rubber specimens were dogbone shaped with nominal dimensions of 69.9 x 4.2 x 9.5 mm and were tested at crosshead speeds of 0.01 mm/mm/min. The rubbery particulate composite specimens were rectangular with typical dimensions of 203.2 x 12.7 x 5.1 mm and were tested at 0.02 mm/mm/min. The bimaterial tests determined the strain rates to be used in these bulk material tests. During the first 10 minutes of deformation, the material strain rates in the bimaterial specimens were approximately constant, and were 0.0030 mm/mm/min and 0.0025 mm/mm/min for the rubber and RPC materials, respectively. These strain rates were matched in the bulk material specimens by the choice of crosshead speed and gage length.

COMPUTATIONAL MODELING

A frequent criticism of computational modeling is that the models are created with insufficient attention given to the accuracy of the properties, geometries, and boundary conditions in the actual application. We hoped to avoid this problem by working closely with the experimental data and by testing the materials to determine the constituent properties. Constitutive materials for both the RPC and the rubber layer were determined.

During the deformation of the specimen, the RPC material experiences relatively small strains and was therefore modeled as linear elastic. This was done using bulk material cut into rectangular specimens as described above, with gage lengths and

crosshead speeds adjusted so that the average strains in the bulk material tests matched those found in the bimaterial specimens. The test data was used for determination of Young's modulus, which was determined as an average for three bulk specimen tests. The constitutive parameters for the finite element model for the RPC material were: Young's modulus = 6.474 MPa and $\nu = 0.499$ (the material is incompressible, so theoretically $\nu = 0.5$, but this causes singularities in the global stiffness matrix).

Modeling the constitutive behavior of the rubber material was more complicated. This material experiences much larger strains during specimen deformation (about 0.7-0.8 mm/mm by the end of the test), so the nonlinear aspects of the problem had to be considered. We used a Ramberg-Osgood curve fit to address the nonlinear behavior of the material. This curve fit is often used to model material with both linear and nonlinear regions in its stress-strain curve. It addresses nonlinearities due to large strains, but does not address the strain rate dependence of the stress-strain curve, a separate issue that may be dealt with in later work.

To determine the Ramberg-Osgood parameters, three dogbone shaped rubber specimens were cut from a sheet, glued into aluminum grips, and tested in a tensile testing apparatus (nominal dimensions were 69.9 x 4.2 x 9.5 mm). We used the average of these three specimen curves for the Ramberg-Osgood curve fit. The procedure followed was to first determine the linear region and the modulus for this region, then to find the yield point. Taking logarithms of the Ramberg-Osgood equation then determines the exponent (see Equation 6 below). The procedure is described effectively in more detail in other works.[7] One noteworthy aspect is that we used the true strains and stresses for the determination. This was done to be consistent with the finite element program, which outputs true strains and stresses rather than engineering strains and stresses. With small deformations, this makes little difference, but the distinction becomes more important with compliant materials experiencing large deformations.

$$\frac{\epsilon}{\epsilon_0} = \frac{\sigma}{\sigma_0} + \alpha\left(\frac{\sigma}{\sigma_0}\right)^m \qquad (6)$$

A thorough determination of the constitutive laws for the two materials would be pointless without also carefully considering the mesh and boundary conditions. Because of this, four meshes of varying levels of refinement were constructed and tested for convergence. The two finest meshes showed no significant difference in any of the respects examined, including overall load vs. displacement response, displacement profiles, and normal strain contours. The final mesh modeled the upper half of the bimaterial specimen using rectangular eight-noded plane stress elements, with a refined region in the rubber layer itself and extending a substantial distance away from it (4.953 mm). Element height in this region was 0.0508 mm. This fine mesh region was connected to a coarse mesh region using the appropriate multi-point constraints. The element aspect ratio in the fine region was low (3.9) and was similar in the coarse region.

Many other aspects of mesh design and element selection were considered and examined to see if they had any bearing on the results. We obtained similar results in all cases. These other aspects include plane stress vs. plane strain elements, reduced vs. full integration, and modeling of the whole specimen rather than just the upper half.

We constructed the boundary conditions to match the experiment. On top surface, the nodes were restricted in the horizontal direction and prescribed vertical displacements were given in 0.254 mm increments (since the experiment crosshead speed was 0.254 mm/min, each step in the finite element analysis formulation represents one minute of deformation). The horizontal restriction simulates the adherence of the upper surface of the bimaterial to a rigid body (here an aluminum grip). Along the line of symmetry (corresponding to the midplane of the specimen), the vertical displacements were constrained. One additional horizontal constraint was added at the middle node along this edge to prevent rigid body translation. The mesh was constructed using the finite element program ABAQUS with nonlinear static analysis options. A summary of the mesh and boundary conditions is depicted schematically in Figure 3.

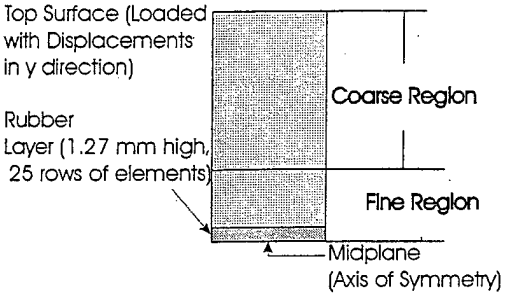

Figure 3: Explanation of Mesh and Boundary Conditions

DISCUSSION

On the most fundamental level, the finite element model of the bimaterial specimen can be visualized as two large linear elastic springs connected by a short nonlinear spring. If the constituent properties are determined well, the overall behavior of the bimaterial experiments and the computational model should agree. The overall load vs. displacements should be compared to verify this, as shown in Figure 4. The figure shows reasonable agreement between the model and the experiment. The slight difference between the two curves is probably caused by using bulk specimen tests to characterize the RPC material. The large blocks of material from which specimens are cut are not always uniform with respect to morphology or properties. Because most of the specimen is RPC material, this deformation dominates the overall specimen deformation. Differences in the bulk-bimaterial properties for the rubber material would affect on the overall load-displacement curve much less.

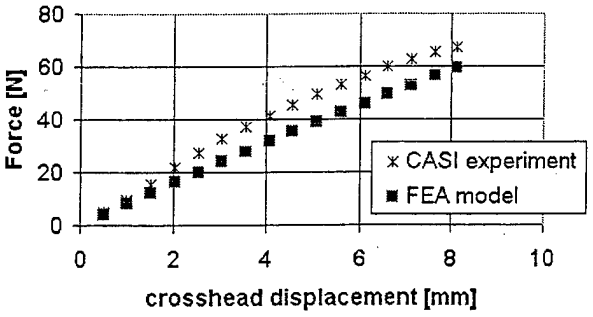

Figure 4: Load vs. Displacements in Experiment and FEA Model

Figure 5 shows an experimental result not shown in the computational model: the presence of five distinct regions in the

bimaterial specimen (i.e., three distinct types of regions, but five distinct regions). The figure shows the vertical component of displacement as a function of instantaneous vertical position (this is the displacement profile mentioned in the Experimental Procedures). Of particular interest is the presence of the interphase regions, where the displacement gradients (and corresponding normal strains ϵ_{yy}) are highest. It is not known at this time what causes this. Further computational model refinement would probably include the use of additional constitutive properties for this region.

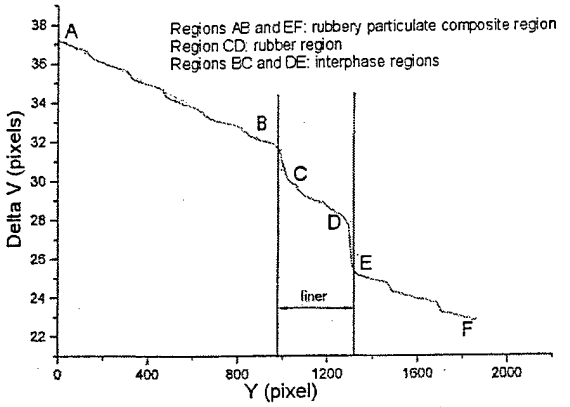

Figure 5: Displacement Profile in Experimental Specimen

The strain vs. time data for each of these regions is shown in Figure 6. The experimental data is shown along with the computational counterpart (because of space limitations, only the Eulerian average strains are shown). The strain rates agree well for the region before substantial debonding of the interface (less than 10 minutes). Later in the tests, the experimental results indicate increasing strain rates for both the rubber layer and the interphase region (strains for the interphase region are not shown here). The absence of the interphase region in the finite element model has already been noted. The increasing strain rates in the liner could be related to this phenomenon, however, more study will be required to decide how to model this feature of the problem.

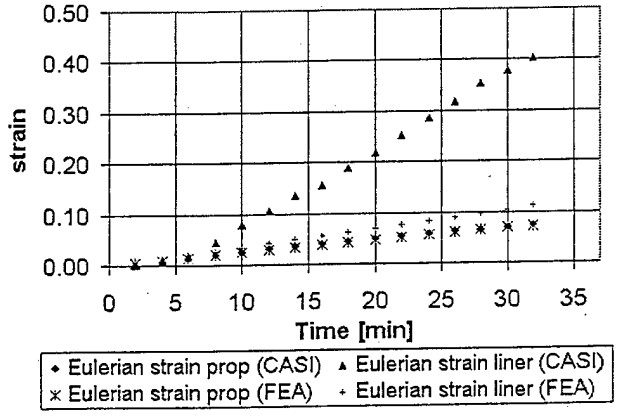

Figure 6: Average Strains vs. Time in the Two Materials

Additionally, the experiments revealed a specimen width effect. During testing, we noted that the width affected the site at which delamination of the interface occurred during the test. The specimens with the width-to-thickness ratio of 2.5 or less delaminated near the center of the specimens, and specimens with the width-to-thickness ratio greater than 2.5 delaminated near the corner (at the intersection of the free surface and the interface) (see Table 1). It should be noted that the bimaterial problem is a three-dimensional problem so this observation may only apply to the specimen thickness tested (5.1 mm). This feature of the problem has not yet been studied computationally.

SUMMARY AND CONCLUSIONS

At this point the results for the experimental and computational results are only tentative; more work will be performed to confirm the phenomena and to examine the causes of the bimaterial specimen behavior. The experimental technique was used to good effect by showing the displacement profiles and the average strains and strain rates in the two materials. This showed the presence of an intermediate region. The strain rates in the RPC were nearly constant throughout the test, but the strain rates in the rubber layer and the interphase region increased during the test. The finite element analysis modeled the overall behavior of the bimaterial specimens well (see Figure 4), but failed to model the interphase region and did not adequately explain the increasing strain rates (Figures 5 and 6). More work will be done on the model to address these issues. A better understanding of the issues presented here will help improve failure predictions in rocket motors, and may have widespread implications in the mechanics of layered materials in general.

The tentative conclusions for this work are:

1. Different behavior is noticed in different regions of the bimaterial specimens. The RPC material experiences fairly uniform strain rates, but the strain rates in the rubber material increase during the specimen deformation.

2. The experimental method shows that the bimaterial specimens have an interphase region that exhibits even higher strains, and that exists in a region between the rubbery particulate composite and the rubber material.

3. The bimaterial specimens delaminate along the interface after about 10 minutes. The location on the interface at which this delamination occurs depends on the width-to-thickness ratio of the specimen, with more narrow specimens exhibiting edge delaminations and wider specimens exhibiting center delaminations.

4. The computational model does not yet address the issues of the interphase region or the increasing strain rates in either the rubber layer or the interphase region.

REFERENCES

[1] Timothy C. Miller and Chi Tsieh Liu. Pressure effects and fracture of a rubbery particulate composite. Experimental Mechanics, 41(3):254–259, 2000.

[2] Chi Tsieh Liu and Timothy C. Miller. Effect of crack size on initiation and growth behavior in a particulate composite material. In Society for Experimental Mechanics IX International Congress and Exposition, pages 1017–1020. Society for Experimental Mechanics, 2000.

[3] Timothy C. Miller. Crack growth rates in a propellant under various conditions. In Proceedings of the 2001 Spring Conference of the Society for Experimental Mechanics, pages 50–53. Society for Experimental Mechanics, 2001.

[4] F. P. Chiang, Q. Wang, and F. Lehman. New developments in full field strain measurements using speckles. In George F. Lucas and David A. Stubbs, editors, ASTM STP 1318. American Society for Testing and Materials, Philadelphia, Pennsylvania, 1997.

[5] D. J. Chen and F. P. Chiang. Computer-aided speckle interferometry using spectral amplitude fringes. Applied Optics, 32(2):225–236, 1993.

[6] D. J. Chen, F. P. Chiang, Y. S. Tan, and H. S. Don. Digital speckle displacement measurement using a complex spectrum method. Applied Optics, 32(11):1839–1849, 1993.

[7] Harmer E. Davis, George E. Troxell, and Clement T. Wiskocil. The Testing and Inspection of Engineering Materials. McGraw Hill Book Co., New York, NY, 3rd edition, 1964.

NTIS DISCLAIMER

❖ This document has been reproduced from the best copy furnished by the sponsoring agency.